Quality Improvement Study

Medicine®

OPEN

Assessment of small hepatocellular carcinoma: perfusion quantification and time-concentration curve evaluation using color-coded and quantitative digital subtraction angiography

Chien-Wei Chen, MD[a,b,c], Li-Sheng Hsu, MD[a,b,d,*], Jun-Cheng Weng, PhD[e,f], Hsu-Huei Weng, MD, PhD[a,b], Yu-Ling Ye, MS[a,b], Sheng-Lung Hsu, MD[a,b], Wei-Ming Lin, MD[a,b]

Abstract

To explore the role of quantitative digital subtraction angiography (QDSA) in the diagnosis of small hepatocellular carcinoma (HCC).

Between November 2015 and November 2017, all patients who underwent chemoembolization for HCC were retrospectively reviewed. Patients with tumors measuring more than 5 cm or evident post-processing imaging artifacts were excluded. Images were post-processed using the QDSA technique. Regions of interest were manually drawn on proper hepatic artery (as a reference), target HCC and peritumoral liver. Time-concentration curves and flow parameters of the peak ratio, subtracted time-to-peak (TTP), and area under the curve (AUC) ratio was obtained and analyzed.

A total of 146 HCCs (mean diameter, 1.6 cm) of 71 cirrhotic patients (54 men, 17 women; mean age, 67.7 years) were enrolled. Compared with liver parenchyma, HCCs showed an increased and more rapid flow (peak ratio, AUC ratio, subtracted TTP, and wash-in slope; all $P < .001$). Compared with untreated HCCs, chemoembolized HCCs showed a slower flow (subtracted TTP and wash-in slope, $P = .004$ and .002, respectively). HCCs with a typical enhancement pattern on computed tomography (CT) or magnetic resonance imaging (MRI) had a trend toward Type III (washout pattern) time-concentration curves ($P < .001$). Chemoembolized HCCs had a trend toward Type II (plateau pattern) time-concentration curves ($P = .005$).

QDSA technology can be used to quantify perfusion measurements of HCC and hepatic parenchyma and to assess perfusion changes after HCC chemoembolization.

Abbreviations: AUC = area under the curve, CT = computed tomography, DSA = digital subtraction angiography, HCC = hepatocellular carcinoma, MRI = magnetic resonance imaging, QDSA = quantitative digital subtraction angiography, ROI = region of interest, TACE = transarterial chemoembolization, TTP = time-to-peak.

Keywords: hemodynamics, hepatocellular carcinoma, liver cirrhosis, perfusion, quantitative digital subtraction angiography, transarterial chemoembolization

1. Introduction

Recent advances in diagnostic technology have allowed the detection of malignant lesions at an earlier stage. Although surgery is considered the optimal management strategy for hepatocellular carcinoma (HCC), curative resection is contraindicated in the care of many patients owing to the poor residual liver function caused by coexisting cirrhosis.[1] Transarterial chemoembolization (TACE) that targets localized small HCC lesions is an option for managing unresectable HCC in patients with advanced cirrhosis.[2] Furthermore, superselective TACE for localized small lesions has a better outcome than whole-liver or lobar TACE, since the therapeutic agent is delivered directly to the target lesions while the embolization of non-targeted normal parenchyma is minimized.[3] However, conventional digital subtraction angiography (DSA) sometimes does not depict small lesions due to cirrhosis-induced irregular enhancement of the background parenchyma. Therefore, the success of TACE in small HCC depends largely on target lesions previously identified with imaging modalities such as computed tomography (CT) and magnetic resonance imaging (MRI).

Recent studies using perfusion CT and MRI have shown potential for quantifying the perfusion of the malignancy and for monitoring the treatment response. However, these tools lack real-time information during TACE.[4,5] C-arm CT has been used to identify HCC and its feeding artery during TACE as well as angiographically occult HCC, with the limitations of a small field of view, additional radiation exposure, and use of a contrast medium.[6] Color-coded and quantitative digital subtraction

Editor: Yan Li.

The authors have no conflicts of interest to disclose.

[a] Department of Diagnostic Radiology, Chang Gung Memorial Hospital Chiayi Branch, Chiayi, [b] Chang Gung University College of Medicine, Taoyuan, [c] Institute of Medicine, Chung Shan Medical University, Taichung, [d] Department of Biomedical Engineering, National Cheng Kung University, Tainan, [e] Department of Medical Imaging and Radiological Sciences, Chang-Gung University, Taoyuan, [f] Department of Psychiatry, Chang Gung Memorial Hospital, Chiayi, Taiwan.

[*] Correspondence: Li-Sheng Hsu, Department of Diagnostic Radiology, Chang Gung Memorial Hospital Chiayi Branch, Chang Gung University College of Medicine, Department of Biomedical Engineering, National Cheng Kung University, No.6, Sec. W., Jiapu Rd., Puzi City, Chiayi County, Taiwan (e-mail: gv107392@yahoo.com.tw).

Medicine (2018) 97:48(e13392)

Received: 17 May 2018 / Accepted: 31 October 2018

http://dx.doi.org/10.1097/MD.0000000000013392

angiography (QDSA) is a technique that uses the syngo iFlow (Siemens, Munich, Germany) software to post-process the data, utilizing all of the images in a given DSA sequence to generate a color map that displays the maximum opacification time and provides time-intensity curves and quantitative flow measurements for a given point or region of interest (ROI).[7]

Color-coded QDSA with whole-liver coverage enables quantitative monitoring of the target lesion without the need for additional contrast medium or radiation dosages. While some QDSA studies have been published, no such study has quantified HCCs in comparison with the background cirrhotic liver.[7–9] The purpose of this study was to report our early experience using color-coded QDSA for perfusion quantification and time-intensity curve evaluation of HCCs, as well as the background cirrhotic liver.

2. Methods

2.1. Patients

Institutional Review Board (IRB) approval was attained for this retrospective study and written informed consents were waived by the IRB. We conducted a retrospective review of all patients who underwent TACE for HCC at our hospital from November 2015 to November 2017. Patients with lack of whole-liver coverage angiogram before TACE, evident artifacts on the post-processed images or large tumors measuring more than 5 cm were excluded. The diagnosis of HCC was confirmed on the basis of the following: previous contrast-enhanced CT or MRI findings, elevated alpha-fetoprotein level, histologic proof or follow-up CT after TACE showing retention of the embolized fragment.

2.2. Angiographic procedures and imaging protocol

All angiographic procedures were performed by 1 of 3 interventionists with 5–11 years of experience. Procedures were performed with an Artis Zee Biplane angiographic system (VC14, Siemens AG, Erlangen, Germany). An angiocatheter (4-French RC1 catheter; Terumo, Tokyo, Japan) was placed in the celiac trunk via a right femoral arterial approach using the Seldinger technique. The imaging parameters were 4 frames per second for 12 seconds. Then, 16 mL of contrast medium (340 mg I/mL) was administered for 4 seconds using a power injector for all subjects. DSA images were acquired in anteroposterior projection.

2.3. Image post-processing and perfusion parameters

All of the DSA images were collected and color-coded using the post-processing software syngo iFlow (Siemens, Munich, Germany), which provides a single image that shows the dynamic movement of the contrast medium through the vessels in color (color-coded single image) for each image pixel. Colors represent early to late contrast flow within a sequence; therefore, the time of the DSA sequence is configurable and can be quantified. Five ROIs (1 on the proper hepatic artery as a reference, 2 on the target HCC, and the other 2 on the peritumoral liver parenchyma for average measurements) were manually drawn by 1 observer, with 2 years of experience as a radiologist, using the minimum caliber (mean, 8.36 mm^2) of the selected vessel as the uniform size of the round ROIs (Fig. 1). Time-concentration curves were obtained for each ROI and divided into 3 types (Fig. 2): Type I curve with a progressive pattern, Type II curve with a plateau pattern, and Type III curve with a washout pattern. The starting time (mean, 1.86 sec) was set as the initial opacification of the vessel. We extracted 3 parameters:

(1) the peak ratio (peak attenuation of the selected ROI in comparison with the reference),
(2) the time-to-peak (TTP) attenuation after injection of the contrast medium, and
(3) the area under the curve (AUC) ratio of the selected ROI in comparison with the reference.

The subtraction method was then used to correct the TTP values (subtracted TTP = TTP of the selected ROI minus TTP of the reference ROI) because the TTP is affected by the distance between the defined ROI and the contrast injection site. The wash-in slope was calculated as the peak enhancement divided by the subtracted TTP.

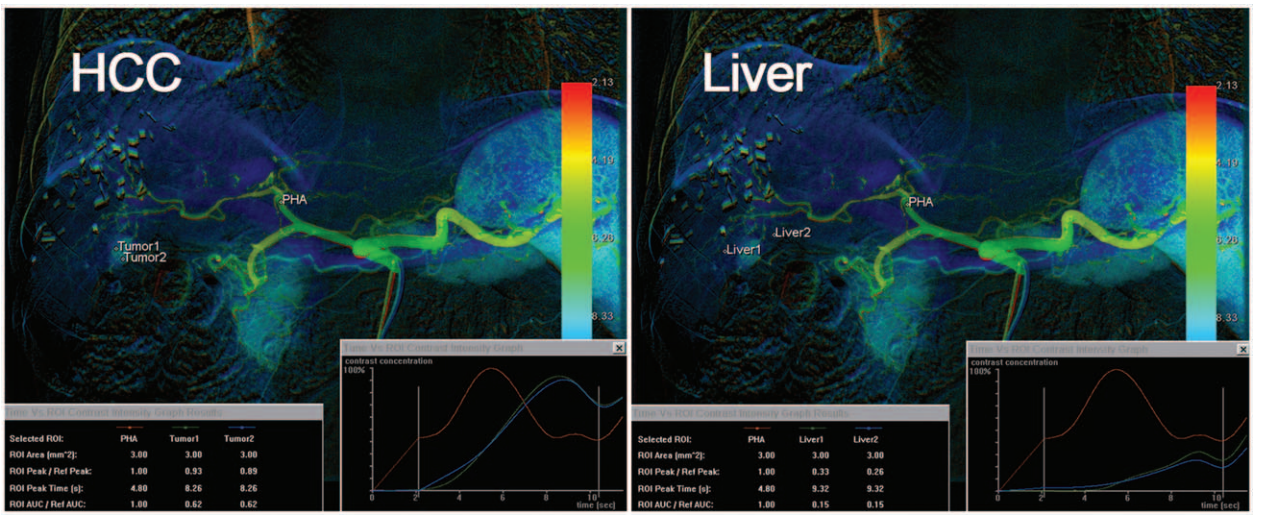

Figure 1. Five regions of interest [ROIs; 1 on the proper hepatic artery as a reference, 2 on the target HCC, and the other 2 on the peritumoral liver parenchyma for average measurements] were manually drawn. Time-concentration curves were obtained for each ROI, along with 3 parameters: the peak ratio, TTP attenuation, and AUC ratio. AUC = area under the curve, HCC = hepatocellular carcinoma, ROI = regions of interest, TTP = time-to-peak.

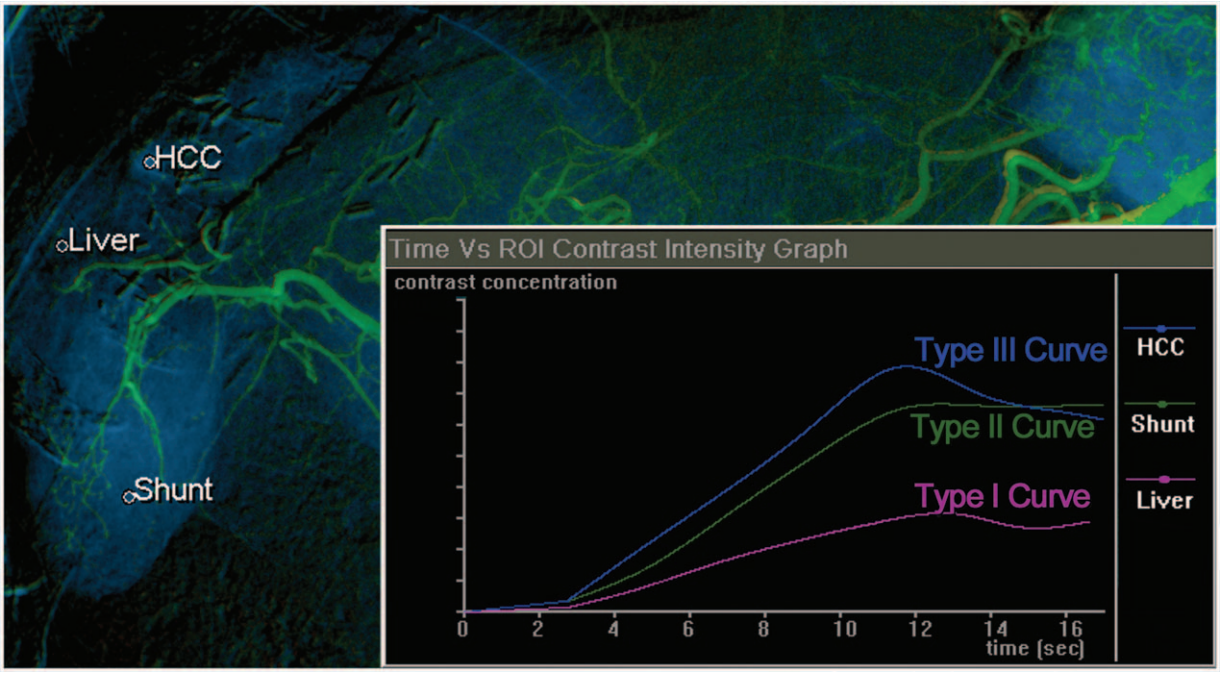

Figure 2. Time-concentration curves were obtained for each ROI and divided into 3 types. The Type I curve (progressive pattern) shows slowly progressive enhancement over time. The Type II curve (plateau pattern) shows relatively rapid enhancement followed by the plateau phase. The Type III curve (washout pattern) shows rapid enhancement followed by the early washout pattern. In this case, cirrhotic liver parenchyma showed a Type I curve and the HCC showed a Type III curve. Angiography also showed a hypervascular lesion in segment 6, which had a Type II curve. Arterioportal shunt was suspected because the follow-up images showed no retention of the embolized fragment after transarterial chemoembolization. HCC = hepatocellular carcinoma.

2.4. Statistical analysis

The estimated parameters of the peak ratio, subtracted TTP, AUC ratio, wash-in slope, and curve type were compared between the HCC and the surrounding cirrhotic liver using the Wilcoxon signed-rank test because the parameters did not follow a normal distribution. The estimated parameters of untreated HCCs were compared with those of treated HCCs after chemoembolization using the Mann–Whitney *U* test. Cross-tabulation analysis was used to compare the relationship between the curve type and imaging diagnosis, as well as the clinical course. Chi-Square test was used to determine whether there was a significant association between the 2 variables. The Cochran-Armitage (CA) trend test was then used to test whether there was a trend toward an association between the 2 variables.

3. Results

A total of 93 patients underwent TACE for HCCs were reviewed. Twenty-seven patients were excluded: 17 patients with lack of whole-liver coveraged angiogram before TACE, 6 patients with evident artifacts on the post-processed images, and 4 patients HCCs measuring more than 5 cm. The study enrolled 146 HCCs (mean diameter, 16.3 mm; range: 5.2–47.1 mm) of 71 patients (54 men, 17 women; mean age, 67.7 years; range: 42–90 years). All of the HCCs were confirmed by imaging studies (33 patients with contrast-enhanced CT and 38 patients with contrast-enhanced MRI) before the TACE procedure. There were 95 typical HCCs (early enhancement with rapid washout) and 51 atypical HCCs (later enhancement without typical washout) based on the CT or MRI imaging findings. Of the total number of HCCs, there were 106 treated HCCs in 49 patients who had previously undergone chemoembolization. Table 1 provides a

Table 1

Baseline characteristics of 146 hepatocellular carcinoma (HCC) lesions in 71 patients.

Characteristic	Value	
patients	**n = 71**	
Age, year	67.7 ± 10.1	(42–90)
Sex		
Male	54	(76.1%)
Female	17	(23.9%)
Liver cirrhosis	69	(97.2%)
HBV carrier only	4	(5.6%)
HCV carrier only	50	(70.4%)
HCV carrier & alcohol abuse	4	(5.6%)
Dual HBV & HCV carrier	8	(11.3%)
Idiopathic (non-B, non-C)	5	(7%)
Child-Pugh class		
Class A	54	(76.1%)
Class B	14	(19.7%)
Class C	3	(4.2%)
HCC Lesions	**n = 146**	
Lesion size, mm		
in CT/MRI	16.3 ± 8.5	(5.2–47.1)
in Angiography	18.4 ± 8.3	(6.3–46.1)
Portal vein thrombosis	8	(5.5%)
Imaging diagnosis*		
Typical HCC	95	(65.1%)
Atypical HCC	51	(34.9%)
Clinical course†		
Untreated HCC	40	(27.4%)
Treated HCC	106	(72.6%)

Note-Value are expressed as Mean ± Standard Deviation (Range), or Number (Percentage).
CT = computed tomography, HBV = hepatitis B, HCC = hepatocellular carcinoma, MRI = magnetic resonance imaging.
* Imaging diagnosis was based on contrast-enhanced CT or MRI before TACE procedure.
† A total of 106 treated HCCs in 49 patients, who underwent chemoembolization before.

Table 2

Estimated parameters of HCCs and of surrounding cirrhotic liver, measured with quantitative digital subtraction angiography (QDSA) technique.

	Peak ratio	Subtracted TTP	AUC ratio	Wash-in slope
Adjacent Liver Parenchyma	0.31 ± 0.17	5.98 ± 1.86	0.22 ± 0.18	0.05 ± 0.03
All HCCs (n = 146)	0.59 ± 0.25	4.22 ± 1.63	0.48 ± 0.24	0.17 ± 0.15
Untreated HCCs (n = 40)	0.59 ± 0.17	3.59 ± 1.25	0.47 ± 0.21	0.18 ± 0.07
Treated HCCs (n = 106)	0.59 ± 0.27	4.46 ± 1.69	0.48 ± 0.25	0.17 ± 0.17
			***P* value**	
All HCCs vs Liver*	<.001‡	<.001‡	<.001‡	<.001‡
Untreated HCCs vs Liver*	<.001‡	.001‡	<.001‡	<.001‡
Treated HCCs vs Liver*	<.001‡	<.001‡	<.001‡	<.001‡
Untreated HCCs vs Treated HCCs†	0.229	0.004‡	0.539	0.002‡

Note-All values except *P* values are expressed as Mean ± Standard Deviation.

AUC = area under the curve, TTP = time-to-peak, HCC = hepatocellular carcinoma.

* Wilcoxon Signed-Rank Test.

† Mann–Whitney *U* test.

‡ If the difference reached statistical significance ($P < .05$).

summary of the baseline characteristics of the patients and HCC lesions.

When compared with the liver parenchyma, HCCs showed an increased and more rapid flow (peak ratio, AUC ratio, TTP, and wash-in slope; all $P < .001$). Subanalysis of the untreated and treated HCCs, in comparison with the liver parenchyma, also showed similar results. Compared with untreated HCCs, chemoembolized HCCs showed a slower flow (subtracted TTP and wash-in slope, $P = .004$ and .002, respectively). Table 2 shows details of the estimated parameters of the HCCs and the surrounding cirrhotic liver, measured using the QDSA technique.

The ROIs of the liver showed an almost Type I (progressive pattern; 96.6%) time-concentration curve. In contrast, the ROIs of the HCCs tended to show Type III (washout pattern; 48.6%) and Type II (plateau pattern; 44.5%) curves. HCCs with a typical enhancement pattern on CT or MRI showed a trend toward Type III curves ($P < .001$). Chemoembolized HCCs had a trend toward Type II (plateau pattern) time-concentration curves ($P = .005$). Results of the cross tabulation analysis of the time-concentration curves and selective ROIs are presented in Table 3.

4. Discussion

Angiogenesis is critical for the progression of HCC. Although it is well known that HCC receives an exclusively arterial blood supply, the majority of well-differentiated HCCs of indistinctly nodular type (early HCCs) receive portal blood supply in addition to the arterial blood supply because they contain portal tracts within the tumor. Many of the small HCCs of indistinctly nodular type show hypovascularity on contrast-enhanced images. Unpaired arteries are sporadic in dysplastic but increased in progressed HCC. Small HCCs of the distinctly nodular type and all of the moderately differentiated HCCs are hypervascular and show "wash-out "on contrast-enhanced images.[10] The abundant arterial perfusion prompts the use of TACE and molecular targeted therapies,[11] and evidence from randomized-controlled clinical trials shows that TACE improves survival in HCC patients.[12] This study confirmed that the arterial flow was increased, and more rapid, in HCC in comparison with cirrhotic liver parenchyma. In addition, this study revealed that chemo-embolized HCCs exhibited slower enhancement (wash-in slope and subtracted TTP) in comparison with untreated HCCs. This is similar to the result of Bachir et al, who reported dynamic contrast-enhanced MRI for the perfusion quantification of HCC.[5] The difference between untreated HCC and chemo-embolized HCC may be due to variable angiogenesis and tumor response to TACE. We thus believe that QDSA provides a useful characterization of angiogenic activity and of HCC response to TACE.

Pathologic angiogenesis appears to be intrinsically associated with the fibrogenic progression of chronic liver diseases, which eventually leads to the development of cirrhosis and related complications, including HCC.[13] However, it may be difficult to distinguish between HCC and atypical hepatocellular neoplasm

Table 3

Cross-tabulation of the time-concentration curves and the selective regions of interest (ROIs), measured with QDSA technique.

	type I curve (progressive pattern)	type II curve (plateau pattern)	type III curve (washout pattern)	Chi-Square test*	CA trend test†
Adjacent Liver Parenchyma	141 (96.6%)	5 (3.4%)	0		
All HCCs (n = 146)	10 (6.8%)	65 (44.5%)	71 (48.6%)		
Typical HCC	0	28 (29.5%)	67 (70.5%)	$P < .001$	$P < .001$
Atypical HCC	10 (19.6%)	37 (72.5%)	4 (7.8%)		
Untreated HCC	0	14 (35%)	26 (65%)	$P = .019$	$P = .005$
Treated HCC	10 (6.8%)	65 (44.5%)	71 (48.6%)		

Note-Values are expressed as Number.

AUC = area under the curve, TTP = time-to-peak, HCC = hepatocellular carcinoma.

* Chi-Square test was used to determine whether there is a significant association between the 2 variables.

† Cochran–Armitage (CA) trend test was used to test where there is a trend association between the 2 variables.

with peliosis in cirrhotic liver.[14] Peliosis hepatis is a rare tumor-like lesion that composed of multiple blood-filled cavities that are difficult to distinguish from other hepatic lesions unless examined by biopsy.[15,16] Imaging characteristic of peliosis hepatis is arterial enhancement without rapid washout,[16] which may be similar to type II (plateau pattern) time-concentration curve in QDSA. In contrast, the HCC tended to show Type III (washout pattern) time-concentration curve. However, this should be verified in a prospective independent study with both QDSA and pathologic correlation.

In the present study, the QDSA technique provided not only quantitative measurements but also time-concentration curves for each selected ROI; the curves were divided into 3 types (Fig. 2), as detailed above. Cirrhotic liver parenchyma presented slowly progressive enhancement over time (Type I curve, 96.6%). In contrast, HCCs tended to show rapid enhancement followed by an early washout pattern (Type III curve, 49.3%) or plateau pattern (Type II curve, 48.6%). These results were in accordance with the diagnostic features of HCC on multiphasic CT or MRI, that is, arterial phase hyperenhancement followed by a portal venous or delayed phase washout appearance.[17,18] The pathophysiological basis for arterial phase hyperenhancement in HCC is well understood, that is, the intranodular arterial supply increases during hepatocarcinogenesis.[19] The mechanisms underlying the washout appearance in HCC are likely informed by several factors, including early venous drainage of the contrast material from the tumor (true washout), progressive enhancement of the background liver (due to the retention of contrast material within the fibrotic parenchyma), and a reduced intranodular portal venous blood supply.[20] In this study, chemoembolized HCCs showed a marginal trend toward hyperenhancement followed by the plateau pattern rather than the washout pattern. The trend toward the plateau pattern can also be explained by a compensatory increase in portal flow after chemoembolization.[5] On conventional DSA, local recurrent HCCs after TACE usually shows obvious tumor staining and necrotic HCC portions showed no tumor staining. This is simple but useful information to judge local tumor recurrence by DSA. The QDSA technique provides a method for extracting more objective quantitative information compared with subjective, qualitative evaluations involving the accumulation of contrast medium during standard DSA. However, this should be verified in an independent prospective study.

The use of the QDSA technique confers several advantages. First, a single field of view, with whole-liver coverage using a single injection of a contrast medium, has been found to be sufficient for post-processing using the QDSA technique. Second, the QDSA technique does not require additional X-ray exposure because DSA acquisition can generate color-coded images and obtain quantitative information. Third, QDSA is a real-time technique. Color-coded images with quantitative measurements are obtained immediately after acquiring the DSA series. Fourth, with QDSA, hemodynamic conditions and changes can be analyzed quantitatively using flow parameters and time-concentration curves.

One of the major limitations of the study is the lack of comparison with metastases or other kind of hepatic neoplasms. In our institution, the diagnosis of most liver tumors is nearly exclusively based on non-invasive imaging modalities, such as ultrasonography, CT, MRI, and molecular imaging. Retrospective data collection for hepatic metastasis is difficult because angiography is not a preliminary diagnostic tool and subsequent TACE is not commonly used to treat hepatic metastasis. Although TACE is also used for metastatic lesions in selective cases,[21] it is rarely used to treat hepatic metastases in our institution. To prove the efficacy of this technique, we should conduct prospective studies in the future to assess the characteristics of various liver tumors, including liver metastases. Second, all enrolled lesions are based on non-invasive criteria for HCC diagnosis, represented by the detection of contrast enhancement with dynamic CT or MR imaging.[22] Pathologic diagnosis was not included in the study and the classification (typical vs. atypical HCC) is histologically improper and probably incorrect. The third limitation of the QDSA technique is that creation of ROI on the DSA image is required to analyze perfusion quantification of target lesions by the Syngo iFlow. Selection of ROI should be avoided over radiopaque object (e.g., retained embolic fragment) or overlapping vessels, as it will cause distortion of measurement result. Therefore, this technique is not suitable for use in patients who are unable to hold their breath. Second, all parameters except the TTP are comparative values (referenced to the Ref-ROI), and thus the absolute blood flow and volume cannot be measured. It is necessary to set a Ref-ROI to calculate the peak and AUC of 1 particular ROI, and the selection of other ROIs also requires strict standardization. A change in the position of the Ref-ROI may affect most of the measurements of the other ROIs. Third, the study cohort was relatively small, which reduces the power to detect meaningful differences between groups. Furthermore, the results of our study were analyzed retrospectively and were not correlated with the long-term clinical outcome. The QDSA technique should be verified in prospective independent studies with long-term follow-up.

In conclusion, color-coding QDSA is a real-time, sensitive, quantitative technique that allows for further hemodynamic evaluation without the requirement additional contrast medium or radiation dosages; however, its full potential remains to be clarified.

Acknowledgments

We thank Mr. Ting Hua for proofreading and statistical support.

Author contributions

Conceptualization: Chien-Wei Chen.
Data curation: Chien-Wei Chen, Yu-Ling Ye.
Formal analysis: Chien-Wei Chen.
Investigation: Chien-Wei Chen, Yu-Ling Ye.
Methodology: Chien-Wei Chen, Yu-Ling Ye.
Software: Chien-Wei Chen, Yu-Ling Ye.
Supervision: Li-Sheng Hsu.
Validation: Li-Sheng Hsu.
Visualization: Li-Sheng Hsu.
Writing – original draft: Chien-Wei Chen.
Writing – review & editing: Li-Sheng Hsu, Jun-Cheng Weng, Hsu-Huei Weng, Sheng-Lung Hsu, Wei-Ming Lin.
Li-Sheng Hsu orcid: 0000-0002-3787-7573.

References

[1] Zaman SN, Johnson PJ, Williams R. Silent cirrhosis in patients with hepatocellular carcinoma. Implications for screening in high-incidence and low-incidence areas. Cancer 1990;65:1607–10.
[2] Matsui O, Kadoya M, Yoshikawa J, et al. Small hepatocellular carcinoma: treatment with subsegmental transcatheter arterial embolization. Radiology 1993;188:79–83.

[3] Itsubo M, Koike K, Tsuno S, et al. Subsegmental transcatheter arterial embolization for small hepatocellular carcinoma. Hepatogastroenterology 2002;49:735–9.
[4] Sahani DV, Holalkere NS, Mueller PR, et al. Advanced hepatocellular carcinoma: CT perfusion of liver and tumor tissue—initial experience. Radiology 2007;243:736–43.
[5] Taouli B, Johnson RS, Hajdu CH, et al. Hepatocellular carcinoma: perfusion quantification with dynamic contrast-enhanced MRI. AJR. Am J Roentgenol 2013;201:795–800.
[6] Iwazawa J, Ohue S, Hashimoto N, et al. Detection of hepatocellular carcinoma: comparison of angiographic C-arm CT and MDCT. AJR. Am J Roentgenol 2010;195:882–7.
[7] Chen CW, Wong HF, Ye YL, et al. Quantitative flow measurement after placing a flow diverter for a distal internal carotid artery aneurysm. J Neurointerv Surg 2017;9:1238–42.
[8] Zhang XB, Zhuang ZG, Ye H, et al. Objective assessment of transcatheter arterial chemoembolization angiographic endpoints: preliminary study of quantitative digital subtraction angiography. J Vasc Interv Radiol JVIR 2013;24:667–71.
[9] Teng MM, Chang FC, Lin CJ, et al. Peritherapeutic Hemodynamic Changes of Carotid Stenting Evaluated with Quantitative DSA in Patients with Carotid Stenosis. Am J Neuroradiol 2016;37:1883–8.
[10] Roskams T, Kojiro M. Pathology of early hepatocellular carcinoma: conventional and molecular diagnosis. Semin Liver Dis 2010;30:17–25.
[11] Zhao GS, Liu Y, Zhang Q, et al. Transarterial chemoembolization combined with Huaier granule for the treatment of primary hepatic carcinoma: safety and efficacy. Medicine 2017;96:e7589. Available at: https://journals.lww.com/md-journal/Fulltext/2017/07210/Transarterial_chemoembolization_combined_with.64.aspx.
[12] Llovet JM, Real MI, Montana X, et al. Arterial embolisation or chemoembolisation versus symptomatic treatment in patients with unresectable hepatocellular carcinoma: a randomised controlled trial. Lancet 2002;359:1734–9.
[13] Bocca C, Novo E, Miglietta A, et al. Angiogenesis and fibrogenesis in chronic liver diseases. Cell Mol Gastroenterol Hepatol 2015;1:477–88.
[14] Gurzu S, Jung I, Contac AO, et al. Atypical hepatocellular neoplasm with peliosis in cirrhotic liver versus hepatocellular carcinoma: a diagnostic trap. Medicine 2015;94:e1189Available at: https://journals.lww.com/md-journal/Fulltext/2015/07040/Atypical_Hepatocellular_Neoplasm_With_Peliosis_in.21.aspx.
[15] Dai YN, Ren ZZ, Song WY, et al. Peliosis hepatis: 2 case reports of a rare liver disorder and its differential diagnosis. Medicine 2017;96:e6471. Available at: https://journals.lww.com/md-journal/Fulltext/2017/03310/Peliosis_hepatis___2_case_reports_of_a_rare_liver.30.aspx.
[16] Iannaccone R, Federle MP, Brancatelli G, et al. Peliosis hepatis: spectrum of imaging findings. AJR. Am J Roentgenol 2006;187:W43–52.
[17] Choi JY, Lee JM, Sirlin CB. CT and MR imaging diagnosis and staging of hepatocellular carcinoma: part I. Development, growth, and spread: key pathologic and imaging aspects. Radiology 2014;272:635–54.
[18] Choi JY, Lee JM, Sirlin CB. CT and MR imaging diagnosis and staging of hepatocellular carcinoma: part II. Extracellular agents, hepatobiliary agents, and ancillary imaging features. Radiology 2014;273:30–50.
[19] Efremidis SC, Hytiroglou P. The multistep process of hepatocarcinogenesis in cirrhosis with imaging correlation. Eur Radiol 2002;12:753–64.
[20] Marrero JA, Hussain HK, Nghiem HV, et al. Improving the prediction of hepatocellular carcinoma in cirrhotic patients with an arterially-enhancing liver mass. Liver Transpl 2005;11:281–9.
[21] Suciu BA, Gurzu S, Marginean L, et al. Significant shrinkage of multifocal liver metastases and long-term survival in a patient with rectal cancer, after trans-arterial chemoembolization (TACE): a case report. Medicine 2015;94:e1848. Available at: https://journals.lww.com/md-journal/Fulltext/2015/10030/Significant_Shrinkage_of_Multifocal_Liver.81.aspx.
[22] Bargellini I, Battaglia V, Bozzi E, et al. Radiological diagnosis of hepatocellular carcinoma. J Hepatocell Carcinoma 2014;1:137–48.